Parameter Estimation of Multiple Non-Linear Damping Sources in Guitar Strings

J.W. CHRISTIAN[1]

Abstract— This paper examines a method used to quantify multiple damping types acting simultaneously on bronze-wound guitar strings. This method involves curve-fitting the time-decay envelopes of filtered string harmonics and using the fitted damping parameters in a single-degree-of-freedom (SDOF) model to verify the results and potentially identify relevant damping design variables for frequency-based damping. Material, aerodynamic, and friction damping are considered in this study, and each type of damping was isolated by changing the environmental conditions. The damping forces from all three types of damping add linearly in the SDOF model, allowing the time decay envelope of each harmonic to be fitted with a function that is a linear summation of each decay function. Both the SDOF model and curve-fitting algorithm could not produce reliable damping coefficients due to summation effects of the three decay functions. It was found that the curve-fitting routine and model solution were most sensitive to the aerodynamic parameter because of the decay function's ability to fit both a steep initial and flat steady-state decay. The test results from vacuum chamber data showed that friction damping comes primarily from the windings on the string rubbing against one another, and that material damping increases linearly with frequency and is proportional to the velocity. Empirically, this gives merit to viscous-like damping as a potential model for material damping.

I. INTRODUCTION

Experienced guitarists can perceive 5% damping variations, and their choice of guitar strings are based on this perception [15]. Some strings are deemed bright and others mellow, but both perceived tones are based on the amount of damping acting on each harmonic. Damping is arguably one of the most important elements of a guitar string, and it is also one of the most elusive design variables. This is primarily due to the absence of a reliable, easy-to-use model that accurately describes the governing damping mechanisms.

The one-dimensional wave equation has been the primary model used to describe the motion of a string; however, it is not a complete model. Different terms have been added to the equation to account for bending stiffness in the string, large amplitude vibrations, wrap-wire windings, damping, and tension modulations. Each equation becomes more complex than the previous, most of which can be solved only using a numerical solver, which requires a large amount of computational power and time. Because the design process is iterative in nature, this model is not of great use to those in a manufacturing setting. It becomes more practical to design a string, quantify the damping, perform another design change, and repeat the process. This leads to another problem: using a damping parameter estimation method that accurately reflects the governing physics.

One popular parameter estimation method involves reconstructing damping matrices for lumped parameter models using experimental modal data. Hasselman outlined a method whereby a proportional, viscous damping matrix could be reconstructed from modal frequencies and knowledge of the mass and stiffness matrices [7]. Minas and Inman performed a similar study in which a non-proportional damping matrix could be reconstructed from incomplete modal frequency information. This study also extended the damping reconstruction method to include a hysteretic damping matrix [9]. Woodhouse and Adhikari performed similar studies in 1998, 2001, 2004, and 2006, in which viscous and non-viscous damping matrices were constructed from complex eigenvalues and eigenvectors and knowledge of the mass and stiffness matrices [12] [2] [3] [13] [14] [1].

The primary limitations of the damping matrix reconstruction method is that knowledge of the mass and stiffness matrices are needed, along with complex eigenvalues and eigenvectors, which are not always easily obtained. Another limitation in this line of study is that an *a priori* assumption must be made regarding which general form the damping term will take on. From this assumed form, the damping coefficients can be calculated; but this generalized damping coefficient matrix in the lumped parameter model often fails to accurately reflect the governing physics occurring in the system. For these reasons, this damping matrix reconstruction method is used primarily in numerical examples and in guitar string synthesis studies.

[1] Manuscript received June 15, 2011. Jonathan Christian, jwchristi at gmail dot com. Research funded in part by D'Addario and Company, Purdue University, and Faurecia Emissions Control Technologies.

Instead of trying to reconstruct a coefficient matrix that describes the damping in a system, other metrics can be used to experimentally quantify the amount of damping on a harmonic basis. One commonly used metric is the logarithmic decrement, a constant that is the ratio of successive peak amplitudes. This metric is useful when applied to a sinusoidal function oscillating at one frequency, but it does not readily describe the appropriate damping mechanism acting on the system. Another metric, known as the quality factor (Q-factor), can be expressed in several ways. The first expression for the Q-factor is the ratio of the maximum dynamic response to static response [4]. When static conditions cannot be measured easily, the Q-factor can be expressed as the ratio of the natural frequency to the half-power bandwidth; this form is also called the system loss factor [5]. In this expression, accurate data near the resonant frequencies are needed. This can often be a problem if two modes have frequencies that are close together. This metric is relatively uninformative unless expressed in the form that Silva used in 2007, in which the Q-factors sum inversely for systems with multiple types of damping. In that study, expressions for each Q-factor were obtained for single-degree-of-freedom systems containing either Coulomb, hysteretic, or amplitude-dependent damping. The net Q-factor was then calculated from the inverse summation of those individual Q-factors, similar to adding capacitors in series [10]. This method shows promise; however, one limitation lies in the fact that those damping measurements are made in the frequency domain, which does not always allow for direct inference into the time-dependent behavior of the damping mechanisms acting on a system.

The last parameter estimation method involves curve-fitting the time-decay envelopes of each harmonic in the system in order to quantify the damping in a system. Smith and Werely performed a numerical study to identify the functions that fit the decay-response of a SDOF system with either Coulomb, quadratic, or viscous damping. Within the expression of each decay function is a damping coefficient which corresponds to the damping force term in the equation of motion. An example of this is shown in equations 1 and 2, below. In Equation 1, the variable ϵ represents the damping coefficient in the equation of motion, which can be calculated using the decay function in Equation 2 to curve-fit the decay-response [11].

$$\ddot{x} + \epsilon|\dot{x}|\dot{x} + {\omega_n}^2 x = 0 \tag{1}$$

$$a_q(t) = \frac{2\pi a_0}{3\pi + 4\epsilon\omega_n a_0 t} \tag{2}$$

It was found that the response of a single, filtered harmonic from a vibrating string was identical to that of a SDOF spring-mass-damper system, giving direct application to the methods described by Smith and Werely.

Several other researchers have performed studies using decay envelope curve-fits to describe damping in an oscillating system. Silva derived general decay functions that reflected the contributions of several types of damping for an oscillating pendulum [9]. The primary limitation in this method is that these generalized curve-fits only geometrically fit the decay profile of an oscillating system while providing little information as to the physics behind the damping mechanisms. Woodhouse used exponential functions to curve-fit the decay profiles of harmonics from a plucked guitar string in order to quantify the amount of damping for each harmonic [13]. One limitation in this study is that not all of the decay profiles could be accurately fitted with an exponential function. This was not a primary concern since the decay rates of these functions were only used to quantify the Q-factor for each harmonic. As mentioned previously, the Q-factor does not provide time-dependent information as to the nature of the damping mechanisms; rather it only quantifies the net damping acting at each harmonic.

The method used in this paper expanded the curve-fitting method used by Smith and Werely and applied it to a real system— a wound guitar string— with multiple types of non-linear damping acting simultaneously. From these curve-fits, the damping coefficients were calculated and used to correlate a SDOF model to match the data so that relevant design variables could be identified to allow for frequency-based damping.

II. Effects of Multiple Damping Types

Smith and Werely gave decay functions related to Coulomb, viscous, and quadratic (aerodynamic) damping each individually acting on a SDOF, spring-mass-damper model. If the damping forces in the equation of motion sum linearly, then the decay envelope of a system with multiple types of damping should be characterized by a linear summation of the individual decay functions defined by Smith and Werely [11]. The equation of motion that defines a system with Coulomb, viscous and aerodynamic damping is shown in Equation 3.

$$\ddot{x} + 2\zeta\omega\dot{x} + \varepsilon|\dot{x}|\dot{x} + \mu[sign(\dot{x})] + \omega^2 x = 0 \tag{3}$$

This equation is normalized by the mass, and ω is the natural frequency; ζ, ε, and μ are the viscous, aerodynamic, and Coulomb damping coefficients, respectively. Note that this equation does not have a material damping term. The energy-loss mechanism for material damping is not well defined and neither is the damping force term in the equation of motion. The energy-loss mechanism is generally referred to as internal friction [9]. Internal friction occurs as the result of internal shear forces created by rows of atoms trying to slide past each other resulting in a time-dependent relationship in which strain lags the stress in a deformed specimen. The most common expression for material damping involves a complex stiffness term; however, this damping model, known as hysteretic damping, is neither physically or mathematically valid. Inaudi and Kelly noted that this type of damping has mathematical conditioning problems which can only be rectified with more numerically intensive equations which are not easy to solve [8]. The author of this paper found that the most common hysteretic damping models either: did not correlate well with real data, resulted in a numerically unstable system, or were impractical to use because of mathematical complexity. Because of these hindrances, a material damping term was not included in the equation of motion and is qualitatively discussed later in this paper.

Equation 1 was solved with the *Odesolve* command in Matlab along with initial conditions of zero initial velocity and a unit displacement at time zero. The time-decay response was curve-fitted with each decay function individually and then fitted with the summation of the three functions given by Smith and Werely and shown below [10].

$$F(t) = \{me^{-at}\} + \left\{\frac{2\pi a_0}{3\pi + ct}\right\} + \{dt + f\} \tag{4}$$

Note that the individual decay functions in Equation 4 are placed in brackets as a visual-aide. As they appear, these decay functions correspond to viscous, aerodynamic, and Coulomb damping respectively. In Equation 4, the following variables were fitted parameters: *m, a, a_0, c, d, f;* and, of these parameters, *a, c, d* correspond to the damping coefficients in Equation 3:

$$\varepsilon = \frac{c}{4\omega} \tag{5}$$

$$\mu = \frac{-\pi\omega d}{2} \tag{6}$$

$$\zeta = \frac{a}{\omega} \tag{7}$$

Figure 1 shows that the linear summation of these decay functions given as Equation 4 accurately describes the time-decay response of a SDOF system with multiple types of damping.

III. Instrumentation

Three different types of steel-core strings were tested in this study. The first string (BW056) had a diameter of 0.056" and had a wrap wire consisting of 80% copper and 20% zinc. A second string (PB056) had the same diameter and a wrap wire with 90–92% copper and 8–10% tin. Qualitatively, musicians comment that the strings with 80% copper sound brighter than those with 90–92% copper [15]. The term "brighter" implies that there is less damping in the higher frequencies. This is examined later in this article to see if the analysis method can verify what the musicians are hearing. The last string tested was the brass-plated core-wire (diameter of 0.02") that was used in both the BW056 and PB056 strings. The core-wire was tested because the material damping was assumed to primarily come from the core-wire, as the wrap wire provided mainly Coulomb damping from the windings rubbing on each other. Because material damping is related to the internal friction forces within the atomic lattice structure, the core-wire was tuned so that it had the same tension as the tuned BW056 string.

In order to isolate the amount of aerodynamic damping acting on the vibrating string, a vacuum chamber was created. A mounting fixture made entirely of steel was used to minimize any dynamic interaction between the string and the boundaries. Frequency response functions obtained from modal testing in all three axes of the nut and saddle showed no dynamic interaction between the mounting structure and the strings. Efforts were made to minimize the energy loss at the boundaries (nut and saddle) to no avail. The strings were clamped at the nut and saddle in order to create a higher mechanical impedance at the boundaries; however, this only added additional

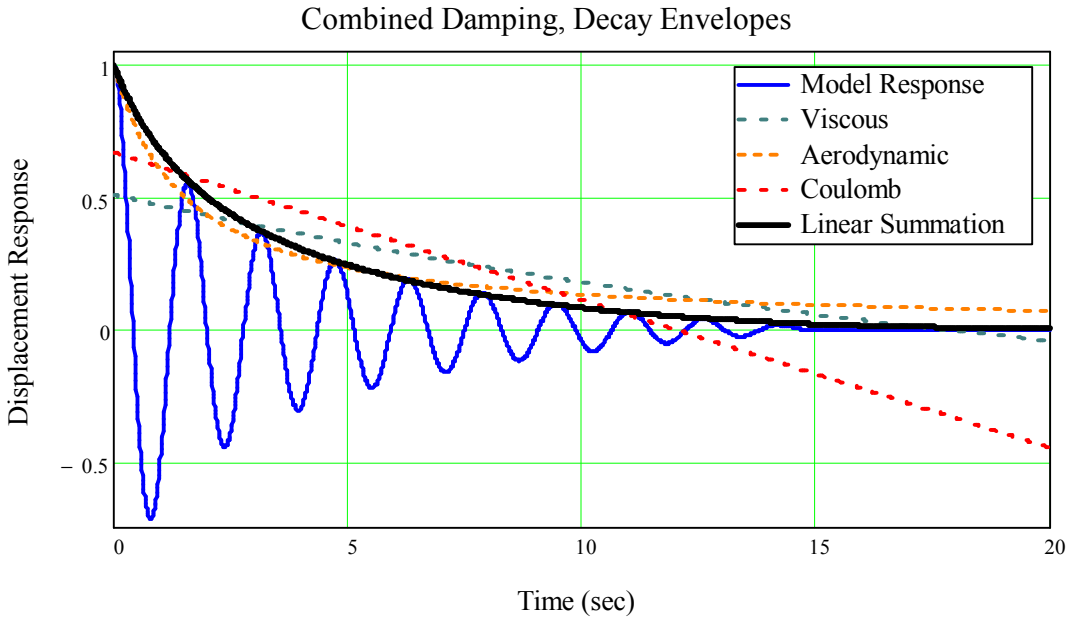

Fig. 1– SDOF Model, Time-Decay Envelope Best-Fit by a Linear Summation of Decay Functions

damping. Lastly, attempts were made to minimize friction energy losses due to the windings of the string rubbing on the nut and saddle by placing materials with low-friction coefficients underneath the string; however, this added additional damping as well. No fluids were used to lubricate the string at the boundaries simply because this would alter the concept of Coulomb damping used in this study. In general, Coulomb damping is defined as energy loss due to dry surfaces coming into contact with one another. For this study, it was concluded that the energy losses at the boundaries were minimal, because no other actions could be taken to minimize energy losses there.

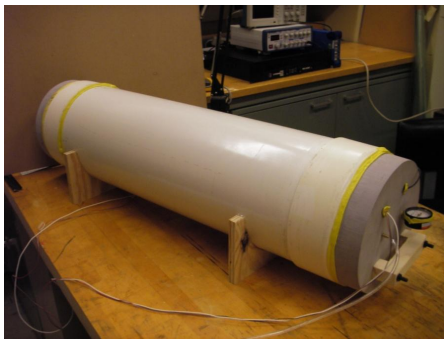

Photo 1 – Vacuum Chamber

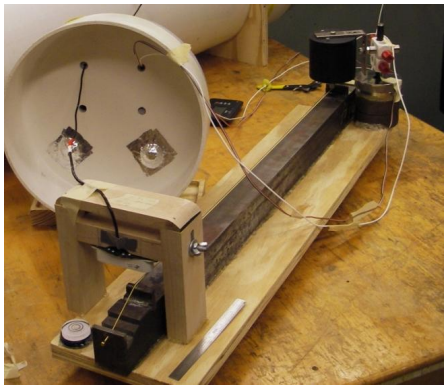

Photo 2 – Mounting Fixture

An electromagnetic pickup with only one magnet was mounted on a wooden fixture above the string and a small electromagnetic shaker with a force gauge attached was used to excite the string. A function generator and amplifier were used to create a repeatable impulse. The pickup and shaker were located 0.8” from the saddle and nut respectively. These positions allowed for high-frequency content to be identified as the first 27 harmonics were easily seen in power spectral density plots. A 20-second time response signal was taken for each string using the shaker and the pickup. Each harmonic was then filtered using a third order, band-pass, Butterworth filter with a bandwidth of 4 Hz and then curve fitted using Equation 4.

IV. Results

Originally it was thought that the viscous damping term in Equation 1 was used by most textbooks out of mathematical convenience because the solutions to the differential equations were easily evaluated and because viscous damping is rarely physically present in most systems. When trying to describe damping from the fluid-structure interaction, the drag force due to air is proportional to the velocity squared as noted by Giordano [6] and Smith and Werely [11]. Because of this, each harmonic was originally curve-fitted with just the aerodynamic and Coulomb decay functions in Equation 4. After the 12th harmonic, it was apparent that the best fit decay function was a pure exponential function; so these higher harmonics were fitted with just an exponential function, while the lower harmonics were fitted with the combined aerodynamic and Coulomb decay functions.

Figures 6 through 11 show the damping parameters and the damping coefficients from these first-pass curve-fits. The damping parameters are the general variables fitted from Equation 4 and the damping coefficients are calculated from these parameters using Equations 5, 6 and 7. In each of these data sets, only a handful of harmonics was fitted, due to the presence of beat frequencies in the filtered harmonics.

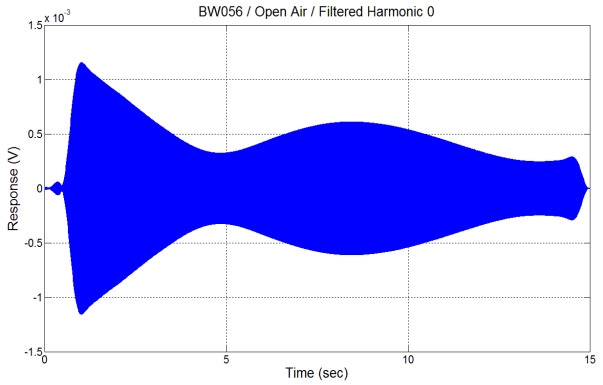

Fig. 2 – BW056, Filtered Harmonic 0

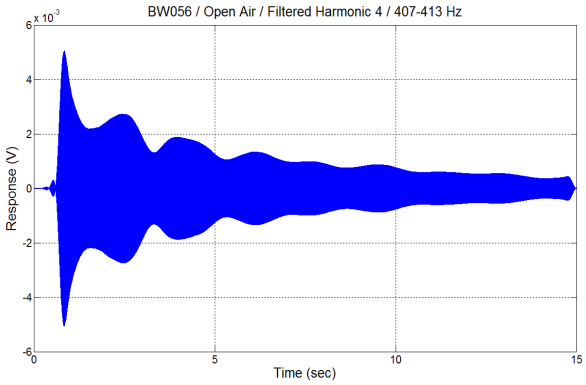

Fig. 3 – BW056, Filtered Harmonic 4

The source of these beat frequencies was from differences in the vertical and lateral modes that were approximately ½ Hz apart. Measurements with a microphone in the vertical and horizontal directions showed two peaks at every harmonic across the entire frequency spectrum in both directions. In the lateral frequency spectrum, the second peak of each harmonic was higher than those seen in the vertical frequency spectrum. This implies that this second peak really was a lateral mode that both the microphone and electromagnetic pickup sensed. From the filtered harmonics, it was discovered that the vertical and lateral modes were also 90° out of phase.

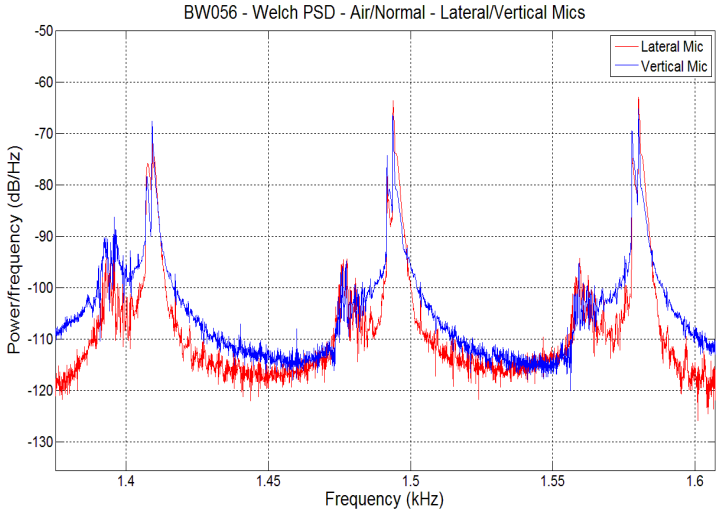

Fig.4 – Vertical and Lateral Power Spectral Density Plots

It was observed that the grooves in the nut and saddle were cut shallower than the recommended depth, and this boundary condition altered the rotational symmetry of the string, allowing for greater motion in the lateral modes. After the string was moved out of the grooves, the split peaks seen across the spectra seemed to disappear. More than likely, the frequencies of the vertical and lateral modes were now closer together and could not be observed due to the frequency resolution. Testing again with the vertical and lateral microphones revealed that even with the string out of the grooves, the frequencies of the vertical and lateral modes were still noticeably different— as much as 0.6 Hz— but the split peaks were now eliminated from both spectrums. For the curve-fits, only the harmonics which showed no influence of

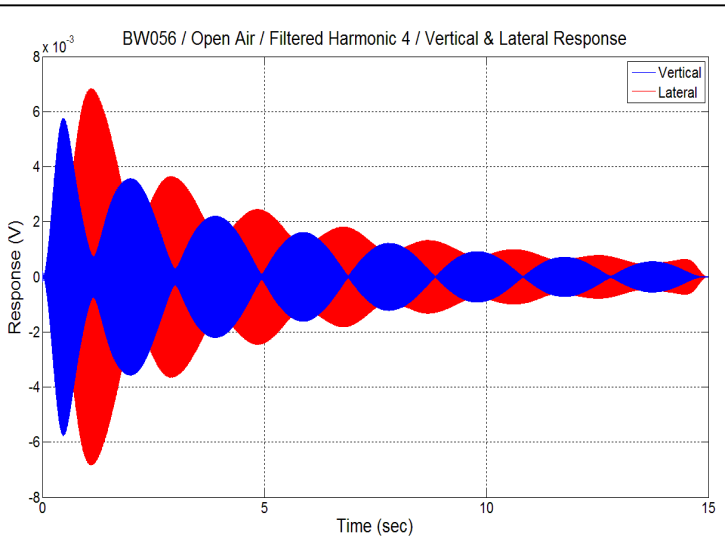

Fig.5 – Lateral Response is 90° Out of Phase with the Vertical Response

beat frequencies were used. Figures 6–11 show the damping parameters and the calculated damping coefficients, as a function of harmonic number, calculated from this first-pass curve-fit.

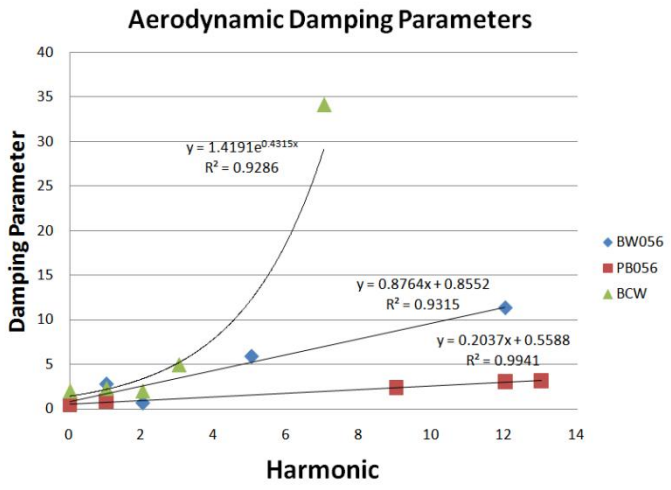

Fig. 6 – Fitted Aerodynamic Damping Parameters

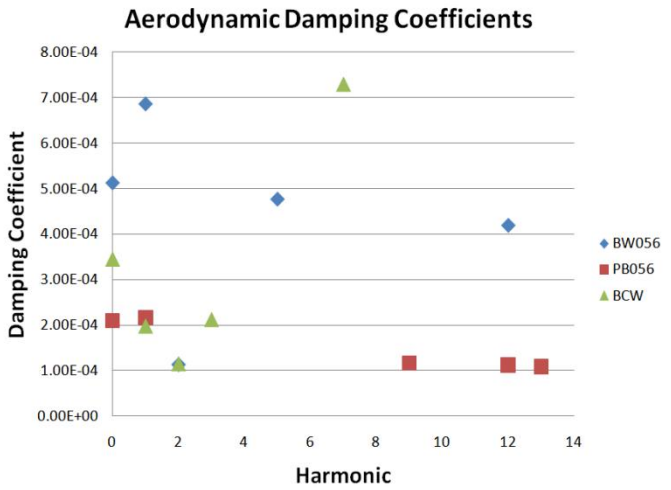

Fig. 7 – Calculated Aerodynamic Damping Coefficients

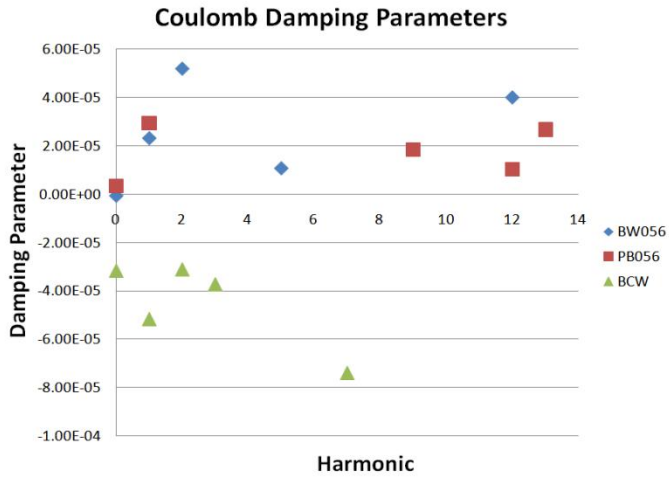

Fig. 8 – Fitted Coulomb Damping Parameters in Air

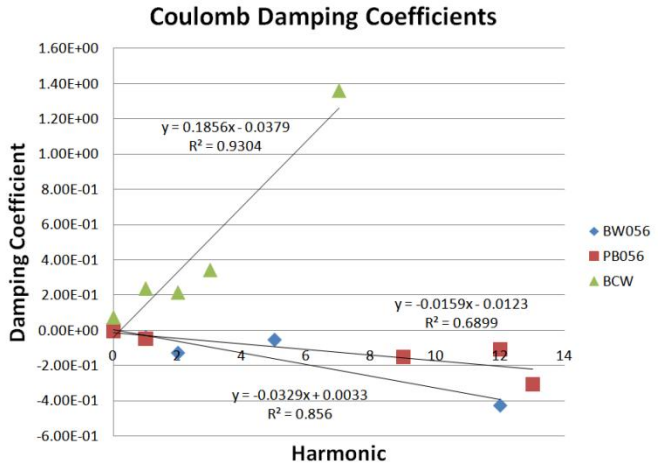

Fig. 9 – Calculated Coulomb Damping Coefficients in Air

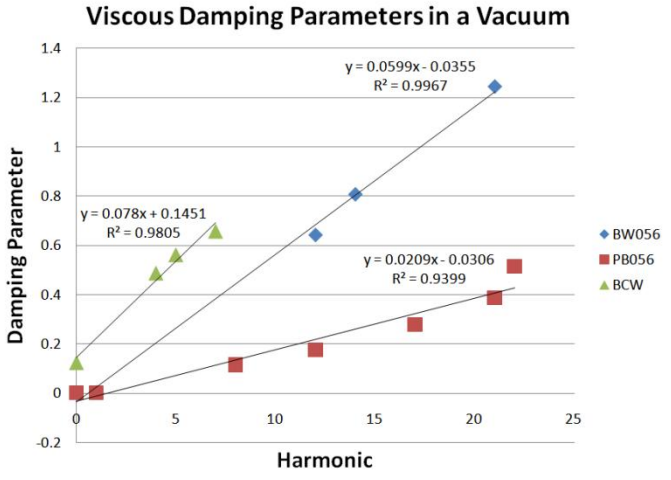

Fig. 10 – Viscous Damping Parameters in a Vacuum

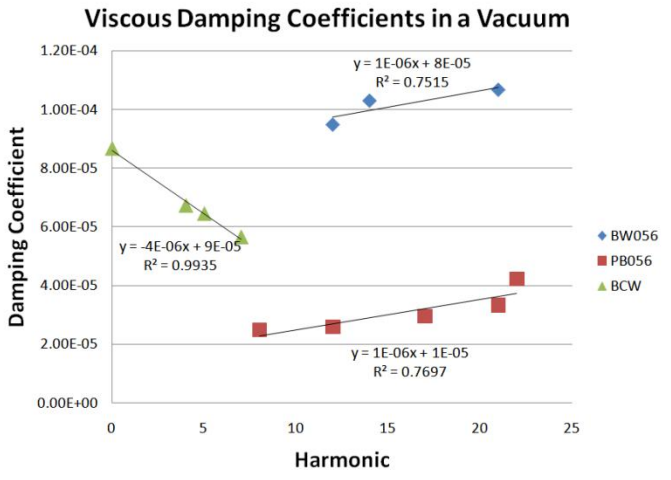

Fig. 11 – Calculated Viscous Damping Coefficients in a Vacuum

From these results, it is difficult to identify trends solely in the damping parameters or the coefficients. Most metrics for measuring damping are normalized by frequency, as is the case for the viscous and aerodynamic damping coefficients. However, because the Coulomb damping coefficient is directly proportional to frequency, the fitted damping parameters may be more informative.

The trends in the damping parameters from the data obtained in a vacuum (see Figure 10) are most interesting. In this data, the viscous damping coefficient and exponential decay were very prominent. Only in the fundamental and first harmonic of the wound strings did the Coulomb damping coefficient contribute to the best-fit decay envelope. Figures 12 and 13 show the linear decay component associated with Coulomb damping.

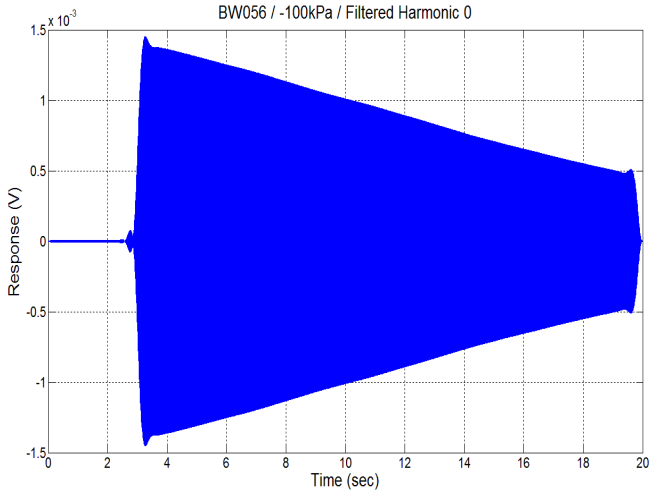

Fig. 12 – BW056, Harmonic 0, Vacuum

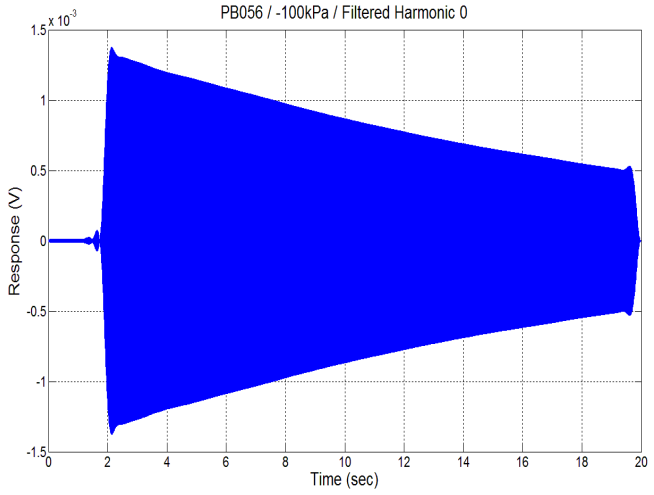

Fig. 13 – PB056, Harmonic 0, Vacuum

After fundamental and first harmonic, the decay function was best characterized with an exponential fit. In the case of the core-wire, each of its harmonics was best fitted with purely an exponential decay function with no contribution of any other type of damping. This implies that the mechanism behind Coulomb damping is the windings of the wrap-wire rubbing together and the source of material damping is in the core-wire. Most important, the vacuum data shows that the viscous damping parameter needs to be considered in every harmonic of the curve fits, as opposed to only in the higher harmonics. The small number of data points in Figures 6–11 is not of concern because the prominence of the viscous damping term indicated that these results needed to be thrown out and re-fitted with all three damping parameters.

In the next round of curve-fitting, the viscous, aerodynamic, and Coulomb terms in Equations 3 and 4 were all used. The table below shows the calculated damping coefficients from this second round of curve-fitting. Curve-fitting the data with all three damping parameters was very difficult, because the curve-fit was most sensitive to only one parameter: the aerodynamic damping parameter. When the aerodynamic damping parameter approached an optimal value, the other damping parameters could vary by as much as 471%. In one curve-fit, an 18% change in the aerodynamic damping parameter caused the Coulomb damping parameter to change by 163%. With these large fluctuations in damping coefficients, the single-degree-of-freedom model was used to see if the calculated damping coefficients actually reflected the physics for each harmonic. Equation 3 was solved using a numerical solver in MathCAD and the experimentally calculated damping coefficients shown in Table 1.

Harmonic	Aerodynamic (ε)	Coulomb (μ)	Viscous (ζ)
0	4.082E-04	-4.272E-03	1.365E-02
1	7.149E-04	-3.570E-02	8.976E-03
12	0	0	9.477E-05
21	0	0	1.039E-04

Table 1 – BW056, Calculated Damping Coefficients from the 2nd Round of Curve-Fits

The solver was equally as sensitive to the aerodynamic damping parameter as in the curve-fit. In order to simulate the response seen in the data, the damping coefficients had to be significantly scaled through an iterative, time-consuming process. Table 2 shows the scaled damping coefficients for the fundamental frequency of the BW056 string. Even though the damping coefficients of the single-degree-of-freedom model had to be significantly scaled, Figure 14 shows that the model decay envelope agreed well with that of the data.

	Aerodynamic (ε)	Coulomb (μ)	Viscous (ζ)
Calculated	4.082E-04	-4.272E-03	1.365E-02
Scaled Value	2.45E-01	2.443E-05	5.573E-05
Scale Factor	600	1/175	1/245

Table 2 – BW056, Harmonic 0, Comparisons of Scaled Damping Coefficients

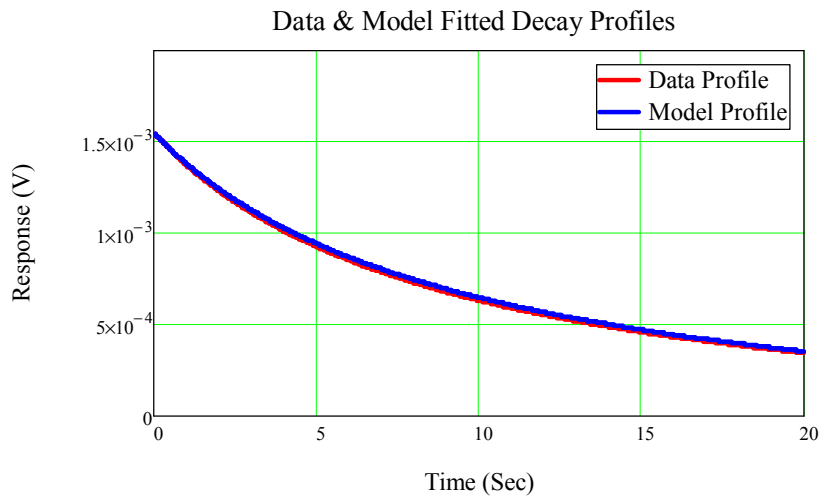

Fig. 14 – Model and Data Decay Responses, BW056 String, Open Air, Harmonic 0

The decay envelope for the fundamental frequency of the model response was then curve-fitted using Equation 4 to see if the damping coefficients from the model matched those calculated from the data. If the calculated model damping coefficients matched those from the data, then this meant that the scaling done earlier was purely out of mathematical convenience to converge the solution.

Table 3 shows that while the model was able to accurately correlate the aerodynamic damping coefficient, it was not able to successfully correlate to the Coulomb and viscous damping coefficients. This method was not continued for any other harmonics, due to three reasons. First, the sensitivity of the curve-fitting algorithm to only one variable showed that the curve-fits may not accurately reflect the physics of the vibrating string, as indicated by the negative Coulomb damping coefficients. Second, even with the scaled damping coefficients, the model was unable to correlate all three damping coefficients from the data. Third, the process to fit the data and match the model with iteratively scaled damping coefficients was very time-consuming which contradicts the goal of creating a method that is simple and easy to use.

	Aerodynamic (ε)	Coulomb (μ)	Viscous (ζ)
Data	4.082E-04	-4.272E-03	1.365E-02
Model	4.17E-04	-1.455E-03	3.8E-02
Difference	2.16%	65.97%	175.02%

Table 3 – Damping Coefficient Comparisons Show Significant Variation

V. Conclusions

This paper shows that for a SDOF system with multiple types of damping, the decay envelope for a string harmonic can be fitted with a function that is a linear summation of the individual decay functions from a representative SDOF model with only one type of damping. Calculating the damping parameters in the time domain is much more informative as to the nature of the damping mechanisms when compared to calculating the Q-factors from the frequency domain. The author successfully expanded upon the curve-fitting and damping parameter calculation method suggested by Smith and Werely [11] and Silva [10], applied it to a real system with multiple types of non-linear damping, and correlated it with a mathematical model. Changing the specimen and ambient conditions allowed for the damping mechanisms to be studied from a physics perspective, rather than a purely mathematical interpretation.

The results from the vacuum tests of a wound string and the core-wire showed that the friction damping acting on a string comes primarily from the windings rubbing on one another. This was proved in that the decay envelopes of every harmonic of the core-wire were purely exponential and showed no contributions of any other type of damping, while the decay envelopes for the BW056 and PB056 strings were a combination of linear and exponential decays. For the wound strings, the fundamental harmonic was purely linear and the first harmonic was a combination of linear and exponential decay; after this, every harmonic was purely exponential. Because linear decay was present in the wound strings, but not the core wire, this indicates that the source of Coulomb damping is in the windings. Because an exponential decay was present exclusively in the core-wire harmonics, and in nearly all of the wound string harmonics, this indicates the source of material damping is in the core-wire.

While the concept of viscous damping was originally thought to be more out of mathematical convenience rather than physical relevance, it is clear from this study that an exponential decay function is relevant in describing the time decay in the system. The vacuum test results show that, in each string, the exponential decay rates of each harmonic increase linearly with frequency, giving merit to a viscous-like damping term. Empirically, this suggests that a simple material damping model may exist.

Although curve-fitting the decay envelopes of each harmonic can be done using a linear summation of the three decay functions, the results cannot be considered reliable due to mathematical summation effects. It is clear that the aerodynamic damping parameter drives both the model and the curve-fit, and this is because of the nature of the decay function. The aerodynamic decay function, which has the form 1/t, has an asymptote at time 0, allowing for a very steep initial decay rate and a very flat response as time approaches infinity. The initial and steady-state decays are the most important parts of fitting the decay envelope and this function can do both well. Because of this, once the aerodynamic damping parameter has been fitted to an optimal value, the other damping parameters are adjusted to make only minor changes to the overall fit. The other damping parameters can take on a wide range of values, because they will not have as large an impact on the overall fit. This validates the concern that the curve-fit shows more mathematical convenience rather than describing the physics acting on the system.

This was confirmed when trying to use the calculated damping coefficients in the mathematical model. The model was also driven by the aerodynamic damping coefficient because of the nature of the solution. While a good visual fit of the fundamental frequency of the BW056 string with three damping types was obtained, the Coulomb and viscous damping coefficients varied by 66 and 175%, respectively. The Coulomb damping coefficients also were the incorrect sign. The negative sign of these coefficients is not physically possible in that negative damping cannot be acting on the system, meaning that the energy-loss mechanism cannot add energy to the system.

VI. Discussion

Many iterations of the curve-fitting and model matching processes had to be done to either adjust scale factors or starting points for initial guesses in fitting the damping parameters. For future study, the curve-fitting and damping coefficient calculations should be repeated for different air pressures. If there is only a change in the aerodynamic damping coefficient as more air is removed from the vacuum chamber, then this will provide valuable insight as to whether the analysis method is more out of mathematical convenience or physical relevance. If the other damping coefficients remain constant in the curve-fits, then this method could actually be describing the physics of the system. However, for now, these results seem to be heavily influenced by mathematical summation effects. Once this obstacle is overcome, this method could become the first step in creating a fast, informative method in which guitar string manufactures can tune a model to achieve frequency based damping.

VII. Acknowledgments

The author would like to thank Professors Mark French, Nancy Denton, and Nick Giordano of Purdue University for their guidance and support of this work. Thanks also to Fan Tao, Ray Keogh, and Jim D'Addario of D'Addario and Company, as well as Shawn Kleinpeter, Gail Guynn, and Tom Rohm of Faurecia Emissions Control Technologies in their sponsorship and support of this work.

VIII. Bibliography

1. Adhikari, S. (2006). Damping modeling using generalized proportional damping, Journal of Sound and Vibration, 293 (1-2), p. 156-170

2. Adhikari, S., & Woodhouse, J. (2001a). Identification of Damping: Part 1, Viscous Damping. Journal of Sound and Vibration, 243 (1), p. 43-61.
3. Adhikari, S., & Woodhouse, J. (2001b). Identification of Damping: Part 2, Non-Viscous Damping. *Journal of Sound and Vibration, 243 (1),* p. 63-88.
4. Beards, C. F. (1996). Structural Vibration: Analysis and Damping. New York, NY: Halsted Press.
5. Ewins, D.J. (2000). *Modal Testing: Theory and Practice (2nd edition)*. Baldock, Hertfordshire, England: Research Studies Press LTD.
6. Giordano, N. (1998). The Physics of Vibrating Strings, *Computers in Physics, 12 (2),* p.138-145
7. Hasselman, T.K. (1972). Method for Constructing a Full Modal Damping Matrix from Experimental Measurements. *AIAA Journal, 10 (4).* p.526-527.
8. Inaudi, J.A., & Kelly, J.M. (1995). Linear Hysteretic Damping and the Hilbert Transform. *Journal of Engineering Mechanics*, 121, p.626-632
9. Minas, C. & Inman, D.J. (1991). Identification of a Nonproportional Damping Matrix from Incomplete Modal Information. *Journal of Vibration and Acoustics, 113, p.219-224.*
10. Silva, C. W. (2007). *Vibration Damping, Control and Design*. Boca Raton, FL: Taylor & Francis Group, LLC.
11. Smith, C.B., & Wereley, N.M. (1999). Nonlinear Damping Identification from Transient Data. *AIAA Journal, 37 (12).* p.1625-1632
12. Woodhouse, J. (1998). Linear Damping Models for Structural Vibration. *Journal of Sound and Vibration, 215 (3),* p. 547-569.
13. Woodhouse, J. (2004a). Plucked Guitar Transients: Comparison of Measurements and Synthesis. *Acta Acustica United with Acustica, 90 (5),* p.945-965
14. Woodhouse, J. (2004b). On the Synthesis of Guitar Plucks. *Acta Acustica United with Acustica, 90 (5),* p.924-944
15. (F. Tao- Research Engineer at D'Addario & Company, personal communication, October 8, 2010).